Title 論文題目	Activated forms of astrocytes with higher GLT-1 expression are associated with cognitive normal subjects with Alzheimer pathology in human brain. (アルツハイマー病理陽性で非認知症であった症例における反応性アストロサイトの形態と GLT-1 発現の解析)
Author(s) 著　者	小林，英司
Degree number 学位記番号	甲第 3019 号
Degree name 学位の種別	博士（医学）
Issue Date 学位取得年月日	2018-03-31
Original Article 原著論文	Scientific Reports 8, Article number: 1712 (2018). doi: 10. 1038/s 41598-018-19442-7
Doc URL	
DOI	
Resource Version	Author Edition

SCIENTIFIC REPORTS

OPEN

Activated forms of astrocytes with higher GLT-1 expression are associated with cognitive normal subjects with Alzheimer pathology in human brain

Received: 23 August 2017
Accepted: 2 January 2018
Published online: 26 January 2018

Eiji Kobayashi[1,2], Masako Nakano[1], Kenta Kubota[1,3], Nobuaki Himuro[4], Shougo Mizoguchi[1], Takako Chikenji[1], Miho Otani[1], Yuka Mizue[1], Kanna Nagaishi[1] & Mineko Fujimiya[1]

Although the cognitive impairment in Alzheimer's disease (AD) is believed to be caused by amyloid-β (Aβ) plaques and neurofibrillary tangles (NFTs), several postmortem studies have reported cognitive normal subjects with AD brain pathology. As the mechanism underlying these discrepancies has not been clarified, we focused the neuroprotective role of astrocytes. After examining 47 donated brains, we classified brains into 3 groups, no AD pathology with no dementia (N-N), AD pathology with no dementia (AD-N), and AD pathology with dementia (AD-D), which represented 41%, 21%, and 38% of brains, respectively. No differences were found in the accumulation of Aβ plaques or NFTs in the entorhinal cortex (EC) between AD-N and AD-D. Number of neurons and synaptic density were increased in AD-N compared to those in AD-D. The astrocytes in AD-N possessed longer or thicker processes, while those in AD-D possessed shorter or thinner processes in layer I/II of the EC. Astrocytes in all layers of the EC in AD-N showed enhanced GLT-1 expression in comparison to those in AD-D. Therefore these activated forms of astrocytes with increased GLT-1 expression may exert beneficial roles in preserving cognitive function, even in the presence of Aβ and NFTs.

Alzheimer's disease (AD) is primarily responsible for dementia, and its dramatic increase in the last decade is a worldwide problem[1]. The neurodegeneration caused by AD is believed to be triggered by an accumulation of amyloid-β (Aβ) plaques and neurofibrillary tangles (NFTs)[2,3]. Aβ plaques induce synaptic dysfunction and neuronal loss due to their toxicity, and also enhance the phosphorylation of tau[4,5]. NFTs are formed by aggregated phosphorylated tau and are involved in neuronal impairment and cell death[6]. Glutamate transmission at synapses is disturbed by the deposition of Aβ and NFTs, and the subsequent elevation in glutamate at axon terminals is associated with cognitive impairment[7].

Although Aβ plaques and NFTs are hallmarks of AD, several postmortem studies have shown the presence of cognitive normal subjects with AD-specific pathological changes in the brain[8,9]. For example, the Medical Research Council Cognitive Function and Aging Study (MRC CFAS) revealed that 34.7% of subjects with massive neuritic plaques in the neocortex showed no dementia[10]. Further, the Nun study found that 32% of subjects with moderate NFT deposition in the neocortex showed no dementia[11]. The reason why AD-specific pathological changes do not cause cognitive impairment is based on differences in the length of education, occupation and mental status in childhood[12–14]; however, the detailed brain mechanisms involved in these discrepancies remain unclear.

[1]Department of Anatomy, Sapporo Medical University, School of Medicine, Sapporo, Hokkaido, 060-8556, Japan. [2]Department of Physical Therapy, Faculty of Human Science, Hokkaido Bunkyo University, Eniwa, Hokkaido, 061-1449, Japan. [3]Department of Physical Therapy, Hokkaido Chitose Rehabilitation University, Chitose, Hokkaido, 066-0055, Japan. [4]Department of Public Health, Sapporo Medical University, School of Medicine, Sapporo, Hokkaido, 060-8556, Japan. Correspondence and requests for materials should be addressed to M.F. (email: fujimiya@sapmed.ac.jp)

Recently it has been reported that cognitive impaired subjects with an AD-specific pathology show a decreased number of neurons and synapses in the hippocampus and cerebral cortex, while cognitive normal subjects with an AD-specific pathology show a constant number of neurons and synaptic integrity in these brain regions[15,16]. In addition, an increased number of astrocytes or microglia was found in cognitive impaired subjects with an AD-specific pathology[15,16], while no such increase was apparent in cognitive normal subjects with an AD-specific pathology. Astrocytes play a number of roles in supporting neurons and maintaining synaptic transmission[17]; however, an accumulation of Aβ plaques stimulate astrocyte conversion to a reactive type that release pro-inflammatory cytokines[18]. In contrast to such harmful reactive astrocytes, beneficial reactive astrocytes that play neuroprotective roles or aid in Aβ clearance in the aged brain were also found[19,20].

We hypothesized that astrocytes in the brain from cognitive normal subjects with an AD-specific pathology might be of the beneficial type that play a neuroprotective role against Aβ and NFT deposition. To clarify this hypothesis, we examined the characteristics of astrocytes in postmortem brains from both cognitive normal and impaired subjects with an AD-specific pathology. The brains were obtained from bodies donated to Sapporo Medical University, and included a variety of cognitive states. We were particularly interested in the amyloid and tau hypothesis as it does not sufficiently explain AD based on the fact that drugs targeting Aβ are not effective in treating cognitive impairment[21]. The results of the present study led us to first propose the brain mechanism involved in maintaining cognitive function despite the progression of AD-specific pathological changes.

Results

Classification of AD neuropathological changes and cognitive function. After elimination of brains on the basis of the exclusion criteria, 51 brains were obtained for this study. We investigated age, years of education, Thal Aβ stage, Braak NFT stage, CERAD neuritic plaque score, and ABC score for each donor and brain (Table 1). For evaluation of neuropathological changes, the "A" and "B" in the "ABC score" were determined from the Aβ deposit- and NFT-affected regions, respectively, as described in Methods. Representative images of each A and B score are shown in Fig. 1a and b, respectively. "C" in the "ABC score" was evaluated from the density of plaques in the neocortex, as described in Methods. Representative images of each C score are shown in Fig. 1c. The overall AD pathological change was diagnosed from a combination of the three scores according to the NIA-AA Regan criteria. Based on these criteria, "Not" and "Low" were regarded as showing no AD pathological change, while "Intermediate" and "High" were regarded as showing AD neuropathological changes (Table 1).

Cognitive function was assessed by postmortem evaluation using the CDR scale. The questions on the CDR were answered by members of the bereaved family or other acquaintances of the donor (Supplementary Table 1). "No dementia" was determined as a CDR score of 0 or 0.5, and "Dementia" was determined as a CDR score of 1, 2 or 3 for convenience as previously reported[22–24]. Based on the AD neuropathological changes and CDR scores, the 51 brains were classified into 4 groups: (1) No AD neuropathological changes with No dementia; N-N, (2) No AD neuropathological changes with Dementia; N-D, (3) AD neuropathological changes with No dementia; AD-N, and (4) AD neuropathological changes with Dementia; AD-D. As the aim of this study was to reveal the neuropathological features that distinguish the AD-N group from the AD-D group, we excluded the N-D group (4 of 51 brains) as this group may have included other neurological deficits such as dementia with Lewy bodies or cerebrovascular dementia. We also evaluated the activities of daily living using the Katz Index and I-ADL score.

We found that 19 of 47 brains (41%) belonged to the N-N group, 10 of 47 (21%) to the AD-N group, and 18 of 47 (38%) to the AD-D group (Table 1). Average age at death was 81.9 ± 7.8 in the N-N group, 87.9 ± 9.1 in the AD-N group, and 91 ± 8.8 in the AD-D group (Table 1). Age at death was significantly higher in the AD-D group than in the N-N group ($P = 0.006$). However, no difference was found between the AD-N and AD-D groups. The causes of death in each group are shown in Supplementary Table 1. Years of education were significantly higher in the N-N group (12.9 ± 3.3) than in the AD-N (9.7 ± 3.5, $P = 0.04$) and AD-D groups (9.5 ± 2.2, $P = 0.01$) (Table 1).

Thal Aβ phase, Braak NFT stage, and CERAD neuritic plaque score were significantly higher in the AD-N and AD-D groups than in the N-N group (Fig. 1d). However, no differences were found between the AD-N and AD-D groups (Fig. 1d). Details of the percentage of each ABC score (A as Thal Aβ phase, B as Braak NFT stage, and C as CERAD neuritic plaque score) in demented and non-demented subjects are shown in Supplementary Table 3. As the entorhinal cortex (EC) is an important area for the evaluation of cognitive function, we investigated neuropathological changes in this area.

The area of the EC. Coronal sections of the brain that cut through the lateral geniculate body and hippocampus are shown in Fig. 2, and the area of the EC (enclosed by red dotted lines in Fig. 2a) was measured. The area was significantly decreased in the AD-D group compared to the N-N group (Fig. 2b). However, no difference was found between the AD-N and AD-D groups (Fig. 2b).

Aβ and PHF-tau in the EC. Aβ-positive area in the EC was significantly higher in the AD-N and AD-D groups than in the N-N group. Likewise, the PHF-tau-positive area in the EC was significantly higher in the AD-N and AD-D groups than in the N-N group (Fig. 3a). However, no differences were found in Aβ- and PHF-tau-positive areas between the AD-N and AD-D groups (Fig. 3a).

The number of NeuN-positive cells and the synaptophysin-positive area in the EC. The number of NeuN-positive cells in the EC was lower in the AD-D group than in the N-N and AD-N groups (Fig. 3b). However, no difference was found in the number of NeuN-positive cells between the N-N and AD-N groups (Fig. 3b). The synaptophysin-positive area was lower in the AD-D group than in the N-N and AD-N groups, however no difference was found between the N-N and AD-N groups (Fig. 3c).

No.	age	sex	Education years	"A" Thal Aβ phase	"B" Braak stage	"C" CERAD score	ABC score	NIA-AA criteria	CDR	Group
1	71	M	20	0	I	None	A0 B1 C0	Not	0	N-N
2	74	M	12	0	I	None	A0 B1 C0	Not	0.5	N-N
3	86	F	8	0	II	None	A0 B1 C0	Not	0	N-N
4	94	F	—	0	I	None	A0 B1 C0	Not	0.5	N-N
5	73	M	—	0	I	None	A0 B1 C0	Not	0	N-N
6	77	M	12	0	IV	None	A0 B2 C0	Not	0	N-N
7	90	M	16	1	IV	None	A1 B2 C0	Low	0	N-N
8	90	M	12	2	II	Moderate	A1 B1 C2	Low	0.5	N-N
9	85	M	12	0	I	None	A0 B1 C0	Not	0.5	N-N
10	88	M	16	0	II	None	A0 B1 C0	Not	0	N-N
11	85	M	12	0	II	None	A0 B1 C0	Not	0	N-N
12	86	M	12	0	III	None	A0 B2 C0	Low	0.5	N-N
13	70	F	12	0	I	None	A0 B1 C0	Not	0	N-N
14	71	M	12	1	I	None	A1 B1 C0	Low	0	N-N
15	79	M	12	0	I	None	A0 B1 C0	Not	0	N-N
16	95	F	6	0	I	None	A0 B1 C0	Not	0	N-N
17	82	M	16	3	I	Moderate	A2 B1 C2	Low	0	N-N
18	80	F	—	0	I	None	A0 B1 C0	Low	0	N-N
19	81	F	16	0	I	None	A0 B1 C0	Not	0	N-N
20	101	F	—	3	IV	Sparse	A2 B2 C1	Intermediate	0	AD-N
21	82	M	12	5	III	None	A3 B2 C0	Intermediate	0.5	AD-N
22	88	F	6	4	IV	Moderate	A3 B2 C2	Intermediate	0	AD-N
23	99	F	8	3	III	Moderate	A2 B2 C2	Intermediate	0.5	AD-N
24	88	M	6	4	V	Frequent	A3 B3 C3	High	0	AD-N
25	77	F	12	2	III	Moderate	A1 B2 C2	Intermediate	0	AD-N
26	89	F	12	3	III	Moderate	A2 B2 C2	Intermediate	0	AD-N
27	98	M	6	3	III	Moderate	A2 B2 C2	Intermediate	0.5	AD-N
28	76	F	9	3	III	Moderate	A2 B2 C2	Intermediate	0	AD-N
29	81	M	16	2	IV	Moderate	A1 B2 C2	Intermediate	0	AD-N
30	92	F	6	5	IV	Frequent	A3 B2 C3	Intermediate	3	AD-D
31	71	F	10	5	IV	Moderate	A3 B2 C2	Intermediate	2	AD-D
32	95	F	10	5	V	Frequent	A3 B3 C3	High	3	AD-D
33	103	F	12	3	VI	Moderate	A2 B3 C2	Intermediate	2	AD-D
34	105	F	—	3	V	Moderate	A2 B3 C2	Intermediate	3	AD-D
35	90	M	8	5	V	Moderate	A3 B3 C2	Intermediate	3	AD-D
36	95	F	12	3	IV	Sparse	A2 B 2C1	Intermediate	3	AD-D
37	85	F	8	3	V	Frequent	A2 B3 C3	Intermediate	2	AD-D
38	91	F	9	3	IV	Frequent	A2 B 2C3	Intermediate	3	AD-D
39	100	F	6	3	III	Moderate	A2 B2 C2	Intermediate	3	AD-D
40	87	M	13	5	III	Moderate	A3 B2 C2	Intermediate	2	AD-D
41	88	M	—	2	III	Moderate	A1 B2 C2	Intermediate	3	AD-D
42	98	M	—	3	IV	Moderate	A2 B2 C2	Intermediate	2	AD-D
43	99	M	9	3	IV	Sparse	A2 B2 C1	Intermediate	3	AD-D
44	90	F	12	3	III	Sparse	A2 B2 C1	Intermediate	1	AD-D
45	76	F	—	3	IV	Moderate	A2 B2 C2	Intermediate	3	AD-D
46	90	M	9	3	III	Moderate	A2 B2 C2	Intermediate	3	AD-D
47	83	M	9	3	III	Moderate	A2 B2 C2	Intermediate	3	AD-D
	N-N:81.9±7.8, AD-N:87.9±9.1, AD-D:91±8.8	M: 24 F: 23	N-N:12.9±3.3, AD-N:9.7±3.5, AD-D:9.5±2.2			None: 16 Sparse 2: Moderate: 22 Frequent: 7		Not:13 Low: 4 Intermediate:28 High:2		N-N: 19 AD-N: 10 AD-D: 18

Table 1. Subject demographics and AD neuropathological changes and cognitive function. CDR = Clinical Dementia Rating scale; N-N = No AD neuropathological changes with no dementia. AD-N = AD neuropathological changes with no dementia; AD-D = AD neuropathological changes with dementia.

The GFAP-positive area, the number of GFAP-positive astrocytes and astrocytic processes in layer I/II of the EC. The GFAP-positive area in layer I/II of the EC was higher in the AD-N and AD-D groups than in the N-N group, however no difference was found between the AD-N and AD-D groups (Fig. 4a). The number of GFAP-positive astrocytes in layer I/II of the EC was higher in the AD-D group than in the N-N and AD-N groups

(Fig. 4a). However, no difference was found in the number of GFAP-positive astrocytes between the N-N and AD-N groups (Fig. 4a). On the other hand, the number of GFAP-positive astrocytic processes was lower in the AD-D group compared to the N-N and AD-N groups (Fig. 4a). No difference was found in the number of GFAP-positive astrocytic processes between the N-N and AD-N groups (Fig. 4a). More characteristically, prominent morphological differences were observed in the astrocytic processes between the AD-N and AD-D groups. The GFAP-positive astrocytes in the AD-N group possessed long, thick, and bushy cytoplasmic processes, while those in the AD-D group possessed relatively short, thin cytoplasmic processes (Fig. 4b). In both the AD-N and AD-D groups, the perikarya was enlarged in comparison to that in the N-N group. In the N-N group, astrocytes were observed as an intermediate or mixed type between those in the AD-N and AD-D groups (Fig. 4b).

The GFAP-positive area, the number of GFAP-positive astrocytes and astrocytic processes in layer III-VI of the EC. The GFAP-positive area in layer III-VI of the EC was higher in the AD-N and AD-D groups than in the N-N group, however no difference was found between the AD-N and AD-D groups (Fig. 5a). The number of GFAP-positive astrocytes and the number of astrocytic processes in layer III-VI of the EC was higher in both the AD-N and AD-D groups than in the N-N groups (Fig. 5a). However, no difference was found in the number of GFAP-positive astrocytes and astrocytic processes between the AD-N and AD-D groups (Fig. 5a). In both the AD-N and AD-D groups, GFAP-positive astrocytes showed enlarged perikarya and thick processes compared to that in the N-N group.

In contrast, no significant difference was found in the number of S100b-positive cells in layer III-VI of the EC, and no significant difference was found in the number of processes of S100b-positive cells among the three groups (Supplementary Figure 4a). Moreover, morphological differences in cell structures between the three groups were not found (Supplementary Figure 4a).

The GLT-1-positive area and mRNA expression in the EC. The GLT-1-positive area in layer I/II of the EC was lower in the AD-D group than in the N-N and AD-N groups (Fig. 4c). However, no difference was found between the N-N and AD-N groups (Fig. 4c). The mRNA expression for GLT-1 in layer I/II of the EC was lower in the AD-D group than in the AD-N group (Supplementary Figure 3). However, no difference was found between the AD-D and N-N groups (Supplementary Figure 3).

The GLT-1-positive area in layer III-VI of the EC was lower in the AD-D group than in the AD-N group (Fig. 5b). However, no difference was found between the AD-D and N-N group (Fig. 5b). The percentage of GLT-1-positive cells in S100b-positive cells in layer III-VI of the EC was higher in the AD-N group than in the N-N and the AD-N groups (Supplementary Figure 4b). However, no difference was found between the AD-D and N-N groups (Supplementary Figure 4b). The GLT-1-positive area in each GLT-1/S100b-positive cell in layer III-VI of the EC was lower in the AD-D group than in the AD-N group (Supplementary Figure 4b). However, no difference was found between the AD-D and N-N groups (Supplementary Figure 4b).

The staining pattern of GLT-1-positive astrocytes varied among the three groups. In the N-N and AD-N groups, the expression of GLT-1 was strong in both the proximal and distal astrocytic processes in layer I/II and layer III-VI, while GLT-1 expression was weaker, especially in the distal astrocytic processes, in the AD-D group (Figs 4c, 5b and Supplementary Figure 4b).

Factors correlated with CDR-SOB. Good correlations were found between the CDR-SOB and Katz index and IADL score as shown in Supplementary Figure 1. In addition, the GLT-1-positive area and the number of GFAP-positive astrocytic processes in the layer I/II showed good correlations with the CDR-SOB, while other factors, including age, area of the EC, Aβ-positive area, number of NeuN-positive cells, synaptophysin-positive area, the GLT-1-positive area and the number of GFAP-positive astrocytic processes in the layer III-VI were moderately or lower correlated with the CDR-SOB (Supplementary Figure 2).

Discussion

To our knowledge, this is the first study to show that reactive astrocytes expressing GLT-1 in the EC are associated with the maintenance of cognitive function in spite of the progression of AD-specific pathological changes. Compared to the AD-D group, astrocytes in layer I/II of the EC from the AD-N group showed an increased number of astrocytic processes and longer or thicker forms with higher GLT-1 expression, while astrocytes in layer III-VI of the EC from the AD-N group showed higher GLT-1 expression. These activated astrocytes in the AD-N group may exert beneficial effects to protect neuronal transmission from the neurotoxicity associated with Aβ and NFT deposition.

We examined brains obtained from bodies aged over 70 years at death donated to Sapporo Medical University. The brain samples used covered various levels of cognitive function and were obtained from donors who died from a variety of causes. After careful exclusion of brains with non-AD neurological diseases such as cerebrovascular dementia or Parkinson's disease-related dementia based on past medical history, we evaluated AD pathology based on the NIA-AA criteria "ABC score" composed of Thal Phase for Aβ plaques, Braak NFT stage and CERAD neuritic plaque score. These criteria are widely accepted as they reflect two important factors associated with AD pathology, Aβ and tau protein deposition[25]. Based on this report, "Not" and "Low" were evaluated as non-AD pathological change, while "Intermediate" and "High" were evaluated as AD pathological change.

To assess cognitive function, the CDR questionnaire was distributed to members of the bereaved families or other acquaintances. CDR is a common method of assessing cognitive function in the elderly, and can be used not only for diagnosis during life but also for postmortem diagnosis[26,27]. The validity and reliability of CDR for postmortem diagnosis were confirmed in a previous report[28], and several clinico-pathological studies have applied this method[15,26]. We evaluated cognitive functions by questionnaires completed by family members but not by

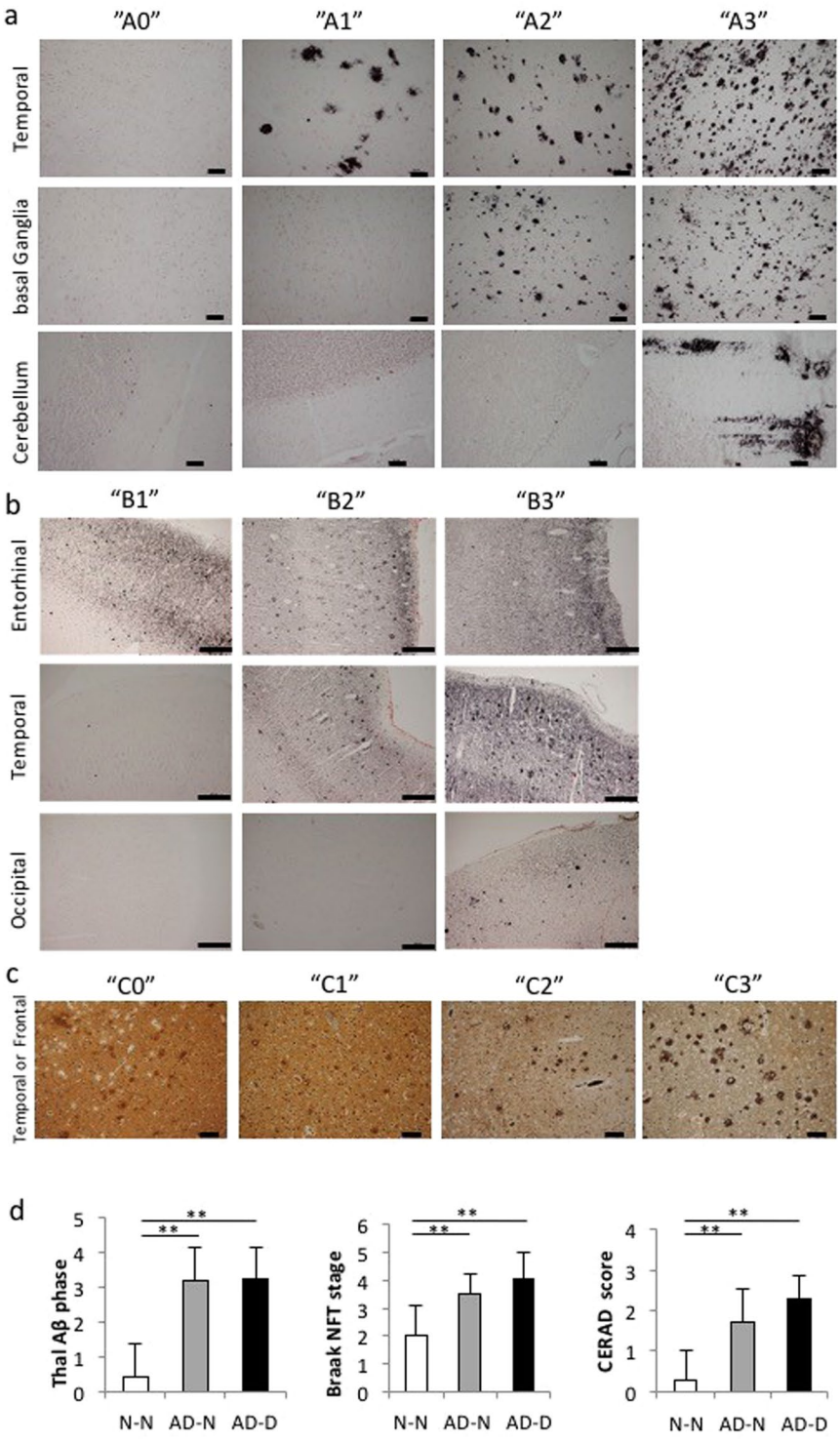

Figure 1. AD neuropathological diagnosis. Representative images of each score for the AD neuropathological changes. (**a**) The "A" score was determined after evaluation of the Thal Phase for Aβ plaques. The figure shows an example of "A0" in which no Aβ deposits are observed in any area, "A1" in which deposits are observed in the temporal area, "A2" in which deposits are observed in the temporal area and basal ganglia, and "A3" in which deposits are observed in the temporal area, basal ganglia and cerebellum (Bar, 100 µm). (**b**) The "B" score was determined after evaluation of the Braak NFT stage. The figure shows an example of "B1" in which the entorhinal region is PHF-tau positive, "B2" in which the entorhinal region and temporal area are PHF-tau positive, and "B3" in which the entorhinal region, and temporal and occipital areas are PHF-tau positive (Bar, 500 µm). (**c**) The "C" score was determined after evaluation of the CERAD neuritic plaque score in the neocortex area by Bielshowsky silver staining. The figure shows an example of "C0" with no neuritic plaques, "C1" with 1 to 5 plaques per 1 mm^2, "C2" with 6 to 20 plaques per 1 mm^2, and "C3" with over 20 plaques per 1 mm^2 (Bar, 100 µm). (**d**) Each score of Thal Aβ phase, Braak NFT stage and CERAD neuritic plaque score is

significantly higher in the AD-N and AD-D groups in comparison with the N-N group. However, no differences are observed between the AD-N and AD-D groups. $^{**}P < 0.01$, Kruskal-Wallis test and Mann-Whitney U test. Values are means ± SD (N-N: n = 19, AD-N: n = 10, AD-D: n = 18).

clinical physicians, as "No dementia" subjects are less likely to take cognitive tests given by clinical physicians when they were alive. In the present study, the cognitive level at 6 months before death was evaluated with CDR 0 (absent) and CDR 0.5 (questionable) classified as "No dementia", and CDR 1, 2, and 3 classified as "Dementia," as previously reported[22–24]. We also evaluated the activities of daily living using the Katz index and I-ADL, and both scores showed a good correlation with CDR, as reported previously[27,29,30]. Moreover, we confirmed the good inter-rater reliability of CDR between two the raters (EK and MN). Thus, the results of CDR were considered reliable.

In this study, the percentage of non-demented subjects with AD pathology was larger than that in previous studies. With regard to the Braak stage, 48% of the subjects with stage III + IV(12 of 25 cases) and 17% of the subjects with stage V + VI (1 of 6 cases) showed no dementia in this study (Supplementary Table 3). On the other hand, 32% of the subjects with stage III + IV and 8% of the subjects with stage V + VI showed no dementia in the Nun study[11]. With regard to the CERAD score, 40% of the subjects with moderate or frequent neuritic plaques (C2 or 3) showed no dementia in this study (10 of 25 cases) (Supplementary Table 3), while 34.7% of the subjects with C2 or 3 showed no dementia in the MRC CFAS study[10]. The discrepancies between the present and previous studies regarding the percentages of subjects with no dementia but with AD pathology might be due to the fact that 57% of the subjects (27 of 47 cases) lived at home during the final 6 months before death and had frequent contact with their family members (Supplementary Table 1, Supplementary Table 2), as a lack social interaction is closely related to the onset of dementia in the elderly[30].

In our study, there were no differences in age or length of education between the AD-N and AD-D groups, and no differences were found in Thal Aβ phase, Braak NFT stage or CERAD score between the two groups. These results indicate that the cognitive impairment in the AD-D group might not be explained by aging, length of education, or deposition of Aβ plaques or tau accumulation in the brain. Therefore, we examined factors other than Aβ plaques and tau accumulation that may cause cognitive impairment in subjects with AD pathology.

The results revealed no differences in the accumulation of Aβ or PHF-tau in the EC between the AD-N and AD-D groups; however, the number of NeuN-positive cells and the area positive for synaptophysin were higher in the AD-N group than in the AD-D group. These results were in agreement with the findings of previous studies in which preserved neuronal number and synaptic density were shown in non-demented subjects with AD pathology[15,16]. As for the hippocampal volume, previous studies have shown that the hippocampal volume is correlated with the neuronal number[31], and a reduction in volume, as assessed by MRI, is used for the diagnosis of AD[32]. Our results showed that the two-dimensional area of the EC was unchanged between the AD-N and AD-D groups, suggesting that the two-dimensional cross-section of the EC, at least, is not correlated with cognitive function.

The most characteristic findings were the differences in the morphology of the astrocytes in layer I/II of the EC between the AD-N and AD-D groups, although both groups exhibited reactive astrocytes with a larger GFAP-positive area than did the N-N group. Astrocytes in the AD-N group possessed longer or thicker processes while those in the AD-D group possessed shorter or thinner processes. Astrocytes located in layers I/II are known as "interlaminar astrocytes" and are characterized by the presence of millimeter-long projections terminating in layer III to IV[33]. It has been reported that in AD patients, disruption of the processes of these interlaminar astrocytes is correlated with dysfunction in neuronal transmission support[34]. In the present study, the longer or thicker astrocytic processes found in layer I/II extended to layer III to IV, where the astrocytic processes may play important roles in the synaptic transmission of neurons connected to the CA1 region[35,36].

In contrast to astrocytes in layer I/II, there were no differences in the morphology of the astrocytes observed in layer III-VI between the AD-N and AD-D groups, although both groups exhibited a larger GFAP-positive area than did the N-N group. Astrocytes in layer III-VI, known as "protoplasmic astrocytes," are spherical and possess several main processes which are accompanied by very thin branches[17]. Therefore, it remains possible that GFAP-positive reactions do not always detect the whole branches of very thin astrocytic processes in layer III-VI. In contrast to GFAP positive astrocytes, there were no differences in both the number of cells and processes in S100b positive astrocytes in layer III-VI. The subpopulation of astrocytes has been reported to be positive for S100b but negative for GFAP[37], and S100b-positive reaction is localized around the perikarya of astrocytes[38]. Therefore, GFAP staining seems to be more suitable for detecting the reactive astrocytes which possess processes than S100b staining.

Reactive astrocytes have also been shown to have diphasic functions[39], including both beneficial effects, such as the formation of a barrier to confine lesions, promotion of blood-brain barrier repair, inhibition of synaptic loss and slowing of neurodegenerative disease progression, and harmful effects, such as the production of reactive oxygen species, secretion of cytokines and inhibition of synapse and axon regeneration[40]. In previous reports, the expression of inflammatory cytokines, such as IL-1β, was higher in demented patients with AD pathology, compared to the non-demented patients with AD pathology[41]. Moreover, a single astrocyte in the human brain is associated with around 2 million synapses via its processes, which support memory formation[42]. Therefore, a diminished number of astrocytic processes leads to reduced glutamate transport and insufficient communication across gap junctions[43].

To clarify the beneficial function of reactive astrocytes in the AD-N group, we examined the expression of GLT-1, which is a major glutamate transporter that uptakes excess glutamate to prevent neuronal excitotoxicity[44,45], in the astrocytes in each group. The GLT-1 expression was detected by immunohistochemistry

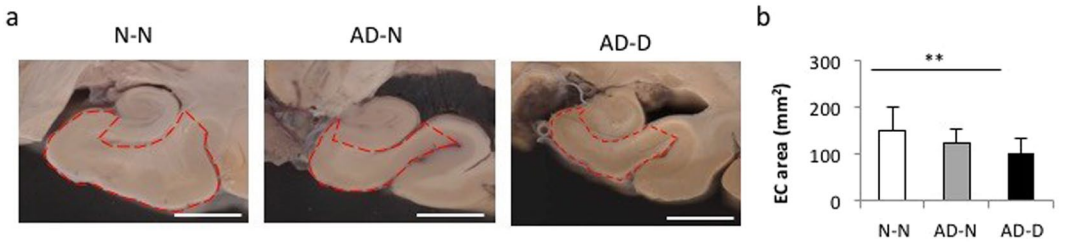

Figure 2. The area of the EC. (**a**) Scanned images of the coronal sections of the brain that cut through the lateral geniculate body and hippocampus are shown (Bar, 10 mm). (**b**) The area of the EC enclosed by red dotted lines is significantly lower in the AD-D group compared to that in the N-N group. No difference is observed between the AD-N and AD-D groups. $^{**}P < 0.01$, one-way ANOVA, Tukey post-test. Values are means ± SD (N-N: n = 19, AD-N: n = 10, AD-D: n = 18).

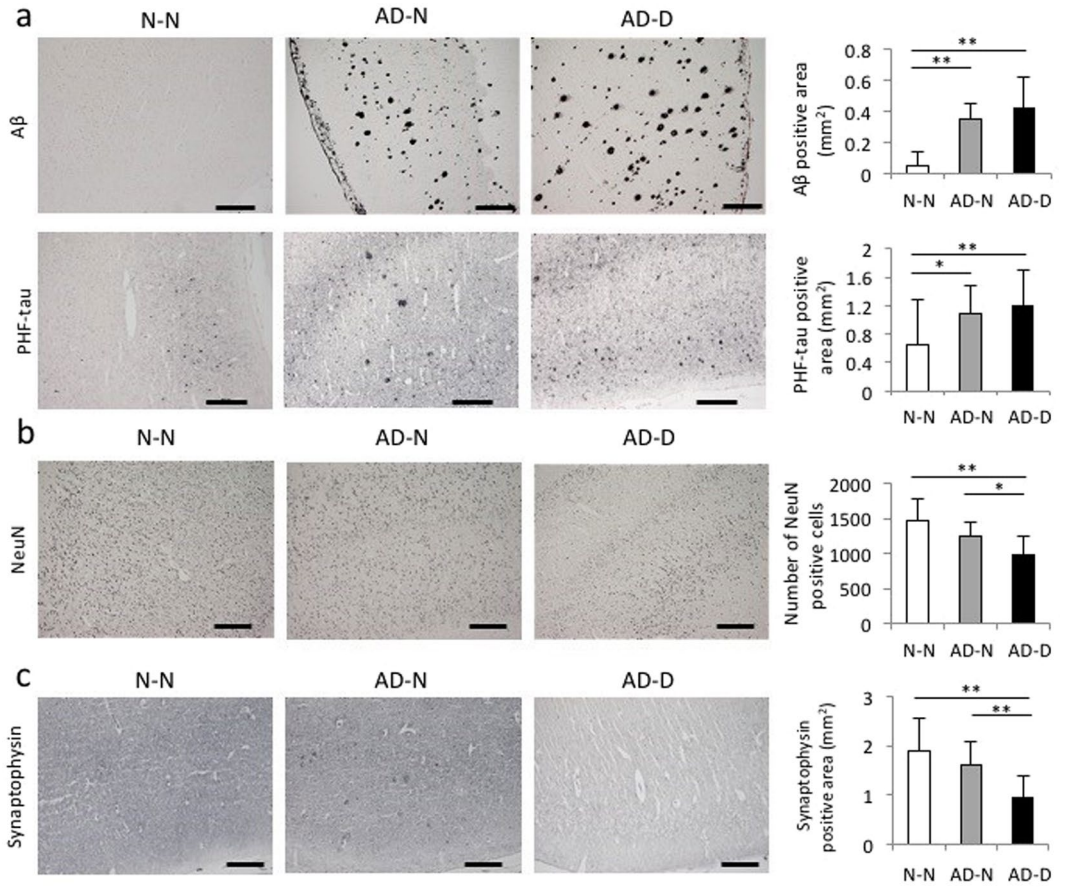

Figure 3. Immunohistochemical analysis of Aβ, PHF-tau, NeuN and synaptophysin in layer I-VI of the EC. (**a**) The Aβ- and PHF-tau-positive area is significantly higher in the AD-N and AD-D groups than in the N-N group. No difference is observed between the AD-N and AD-D groups (Bar, 500 μm). (**b**) The number of NeuN-positive cells in the EC is lower in the AD-D group compared to those in the N-N and AD-N groups. No difference is observed found in the number of NeuN-positive cells between the N-N and AD-N groups (Bar, 500 μm). (**c**) The synaptophysin-positive area is lower in the AD-D group than in the N-N and AD-N groups. No difference is observed between the N-N and AD-N groups (Bar, 500 μm). $^{*}P < 0.05$, $^{**}P < 0.01$, one-way ANOVA, Tukey post-test. Values are means ± SD (N-N: n = 19, AD-N: n = 10, AD-D: n = 18).

and its validity was confirmed by a quantitative RT-PCR. We observed a higher level of GLT-1 expression in astrocytes in the AD-N group compared to that in the AD-D group in both layer I/II and layer III-VI, suggesting that astrocytes in the AD-N group play beneficial roles in neuronal functions. The discrepancies in GLT-1 expression and morphology between astrocytes in the AD-N and AD-D groups in layer III-VI can be explained by the fact that astrocytes in the AD-N groups express high levels of GLT-1 in the very thin

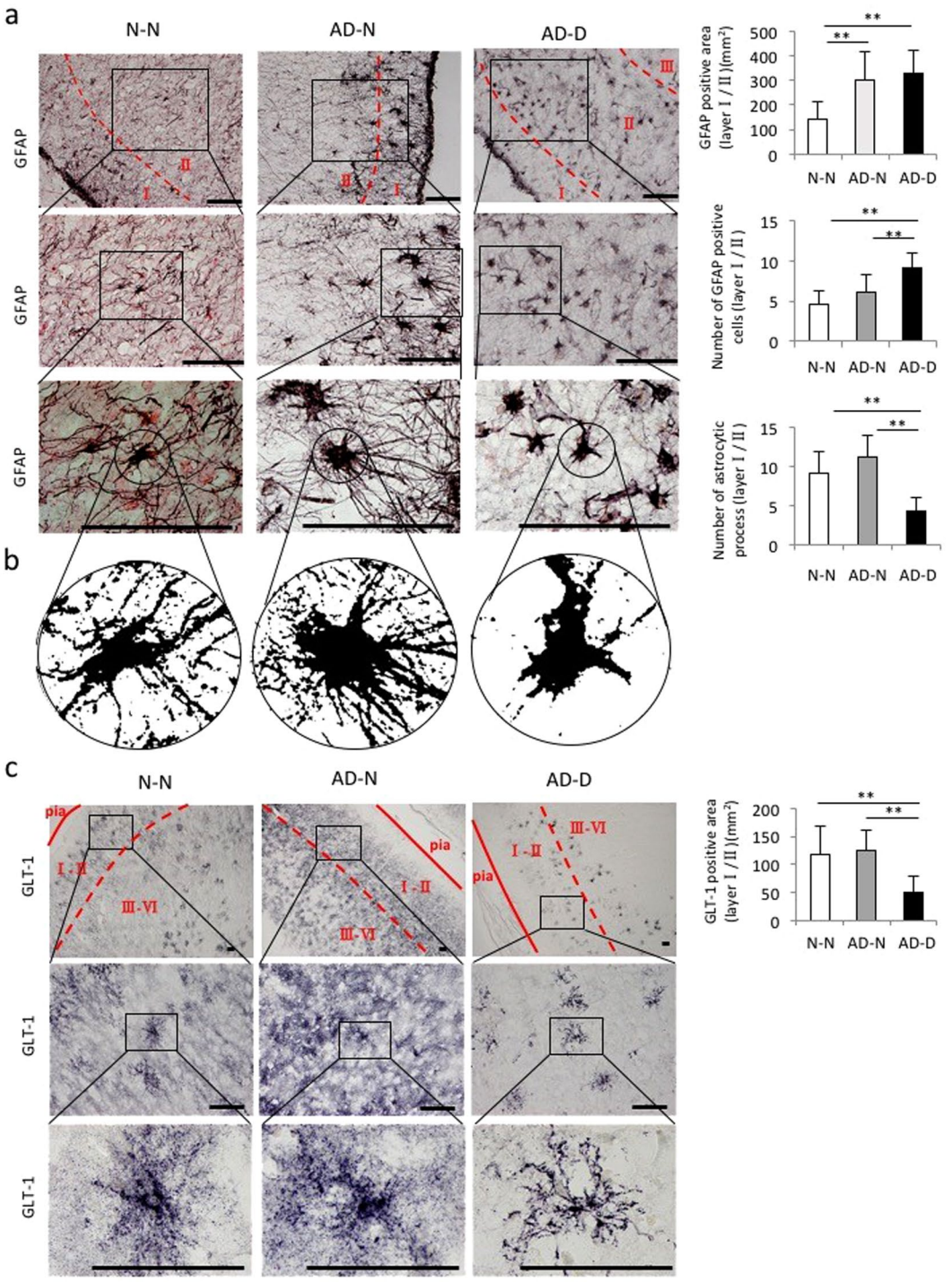

Figure 4. Immunohistochemical analysis of GFAP and GLT-1 in layer I/II of EC. (**a**) Images of GFAP-positive astrocytes shown at different magnifications (Bar = 100 μm). The GFAP-positive area is higher in the AD-N and AD-D groups than in the N-N group, while no difference is observed between the AD-N and AD-D groups. The number of GFAP-positive astrocytes is higher in AD-D group than in the N-N and AD-N groups, while no difference is observed between the N-N and AD-N groups. Astrocytic processes in the AD-N group appear extremely long, thick, and bushy, while those in the AD-D group appear short and thin. (**b**) The number of astrocytic processes observed 20 μm away from the soma is lower in the AD-D group than in the N-N and AD-N groups. (**c**) GLT-1 images are shown at different magnifications (Bar = 100 μm). The GLT-1-positive area is lower in the AD-D group than in the N-N and AD-N groups, while no difference is observed between the N-N and AD-N groups. The expression of GLT-1 is strong in both the proximal and distal astrocytic processes in the N-N and AD-N groups, while GLT-1 expression is weaker, especially in the distal astrocytic processes, in the AD-D group. $^{**}P < 0.01$, one-way ANOVA, Tukey post-test. Values are means ± SD (N-N: n = 19, AD-N: n=10, AD-D: n = 18).

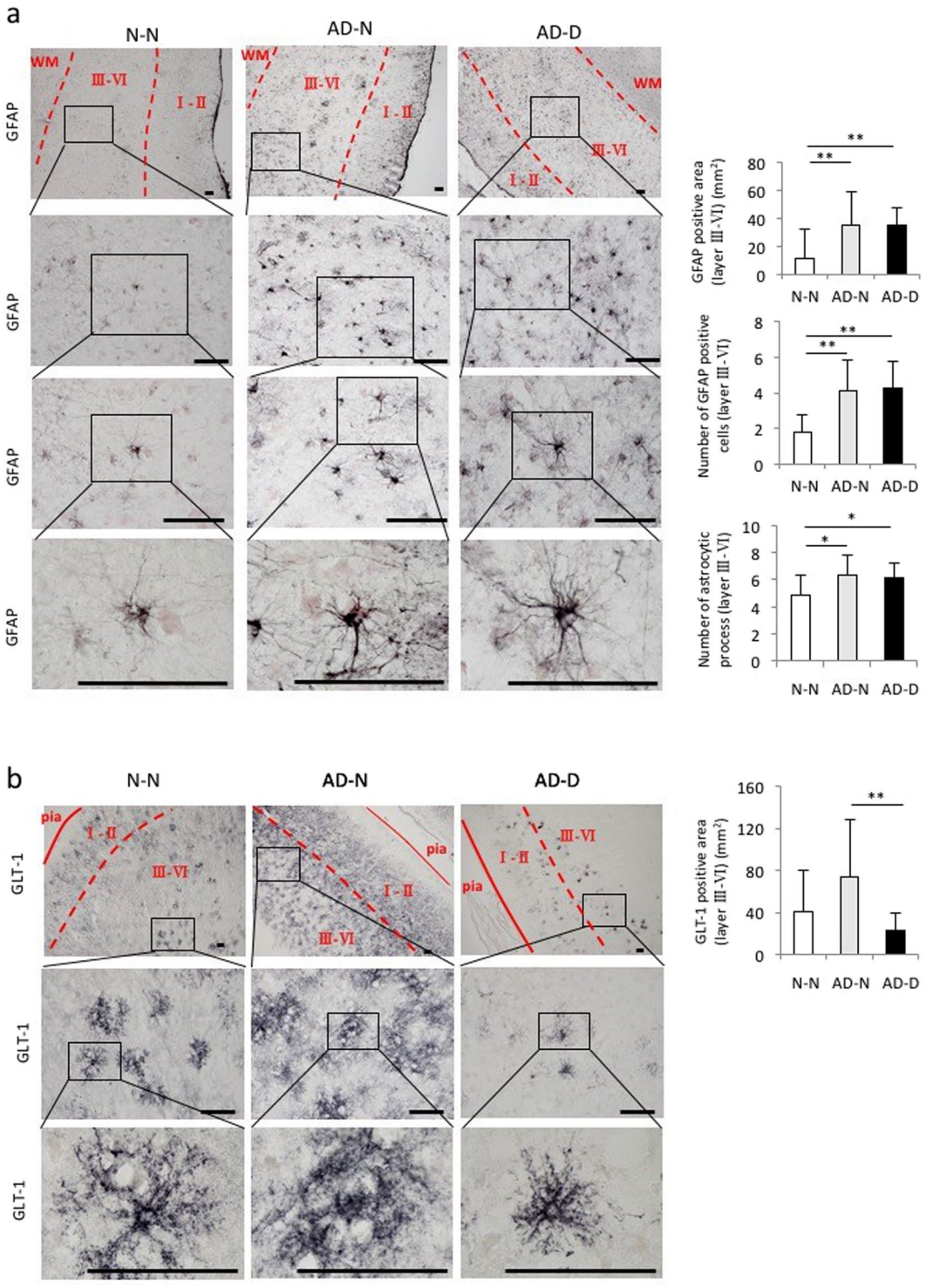

Figure 5. Immunohistochemical analysis of GFAP and GLT-1 in layer III-VI of EC. (**a**) Images of GFAP-positive astrocytes shown at different magnifications (Bar = 100 μm). The GFAP-positive area is higher in the AD-N and AD-D groups than in the N-N group, while no difference is observed between the AD-N and AD-D groups. The number of GFAP-positive astrocytes is higher in AD-N group and AD-D than in the N-N group, while no difference is observed between the AD-N and AD-D groups. The number of astrocytic processes observed 20 μm away from the soma is higher in the AD-N and AD-D groups than in the N-N group. (**b**) GLT-1 images are shown at different magnifications (Bar = 100 μm). The GLT-1-positive area is lower in the AD-D group than in the AD-N groups. The expression of GLT-1 is strong in both the proximal and distal astrocytic processes in the AD-N groups, while GLT-1 expression is weaker, especially in the distal astrocytic processes, in the AD-D group. $^{*}P < 0.05$, $^{**}P < 0.01$, one-way ANOVA, Tukey post-test. Values are means ± SD (N-N: n=19, AD-N: n = 10, AD-D: n = 18).

processes, but they were not detected completely by GFAP immunohistochemistry[46]. The higher expression of GLT-1 in astrocytes in layer III-VI from AD-N group was also confirmed by the overlapping staining of GLT-1 and S100b. In fact, the percentages of GLT-1-positive cells in S100b-positive cells and GLT-1 expression in each cell were higher in the AD-N group than in the N-N and the AD-N groups. Previous studies have shown that a reduction in GLT-1 is related with the cognitive impairment in AD[47,48], and functional abnormalities in GLT-1 induce synaptic loss[49]. In the present study, reactive astrocytes in the AD-D group showed weak GLT-1 expression in spite of a higher number of cells, suggesting that these reactive astrocytes may not function adequately in the brain.

Various factors are known to influence the number of astrocytic processes as well as GLT-1 expression; for example, the ramification of astrocytic processes is increased by physical exercise or an enriched environment[50,51], and GLT-1 expression is up-regulated by treadmill training[52]. Furthermore, GLT-1 expression and the number of astrocytic processes are increased through the memory formation processes[53]. Although the details of daily life and intellectual activity of the donors in the present study were not known, the potential for reactive astrocytes to be converted from non-activated to activated type and the maintenance of GLT-1 expression might be key factors in the preservation of normal cognitive function, even in the presence of AD pathology.

In conclusion, activated forms of astrocytes with higher GLT-1 expression are associated with cognitive normal subjects with the AD pathology in the brain. Identification of methods to convert reactive astrocytes into this beneficial type appears to afford a promising approach to the prevention of AD.

Methods

Subjects. All brains were obtained from the body donation program run by the Sapporo Medical University (Shiragiku-kai). This program consists of members aged 70 years or older who donate their bodies for medical education and research after death. The donation was agreed to by the members while they are alive. There were no prisoners in the subjects of this study. The protocols were approved by the Sapporo Medical University Ethics Committee and informed consent was obtained from all participants. All study methods were performed in accordance with the relevant guidelines and regulations of Sapporo Medical University.

Cognitive function was assessed by postmortem evaluation of informant questionnaires as reported previously[28]. The questionnaires consisted of the Japanese version of the Clinical Dementia Rating Scale (CDR)[22,24,54], Katz Index[55] and I-ADL[56]. Details of CDR are described in Supplementary information.

AD neuropathological diagnosis. For evaluation of AD neuropathological changes, we applied three assessment scales: the Thal Phase for Aβ plaques[57], Braak NFT stage[58,59] and CERAD neuritic plaque score[60]. Details of evaluation of each score are described in Supplementary information.

After assessing each score of the "ABC", we classified each brain as "Not", "Low", "Intermediate" or "High" based on a combination of the three scores according to guidelines of National Institute on Aging-Alzheimer's Association[25]. "Not" and "Low" corresponded to no AD neuropathological change, while "Intermediate" and "High" corresponded to AD neuropathological change. These procedures were applied to each brain with the assessors blinded to the donor.

Immunohistochemistry. Whole brain samples were fixed in 10% formalin. Blocks of the target area were cut, and then immersed in 15% sucrose solutions. For immunohistochemical analysis, coronal sections were cut into 20 μm thick frozen sections and obtained every 100 μm. A standard avidin-biotin complex (ABC) method was used for the analysis. Details of antibodies are described in Supplementary information.

Statistical analysis. One-way ANOVA followed by Tukey post hoc comparison was used to detect differences among the three groups for variables with normal distributions. Non-parametric Kruskal-Wallis test and Mann-Whitney U test were used to detect differences among groups for variables with non-normal distributions. Bartlett's test was used to confirm the data distributions. Spearmann's correlation coefficient was used to confirm correlations between the CDR-SOB and Katz Index, I-ADL, age, area of the EC, Aβ-positive area, PHF-tau-positive area, number of NeuN-positive cells and synaptophysin-positive area. Statistical significance was set at 5% and data are presented as mean ± standard deviation (SD). All statistical analyses were performed using R software (version 3.3.2).

References

1. Cornutiu, G. The Epidemiological Scale of Alzheimer's Disease. *J Clin Med Res* **7**, 657–666 (2015).
2. Hardy, J. & Selkoe, D. J. The amyloid hypothesis of Alzheimer's disease: progress and problems on the road to therapeutics. *Science* **297**, 353–356 (2002).
3. Querfurth, H. W. & LaFerla, F. M. Alzheimer's disease. *N Engl J Med* **362**, 329–344 (2010).
4. Mucke, L. & Selkoe, D. J. Neurotoxicity of amyloid beta-protein: synaptic and network dysfunction. *Cold Spring Harb Perspect Med* **2**, a006338 (2012).
5. Shankar, G. M. & Walsh, D. M. Alzheimer's disease: synaptic dysfunction and Abeta. *Mol Neurodegener* **4**, 48 (2009).
6. Iqbal, K., Liu, F., Gong, C. X. & Grundke-Iqbal, I. Tau in Alzheimer disease and related tauopathies. *Curr Alzheimer Res* **7**, 656–664 (2010).
7. Danysz, W. & Parsons, C. G. Alzheimer's disease, beta-amyloid, glutamate, NMDA receptors and memantine–searching for the connections. *Br J Pharmacol* **167**, 324–352 (2012).
8. Katzman, R. *et al*. Clinical, pathological, and neurochemical changes in dementia: a subgroup with preserved mental status and numerous neocortical plaques. *Ann Neurol* **23**, 138–144 (1988).
9. Price, J. L. & Morris, J. C. Tangles and plaques in nondemented aging and "preclinical" Alzheimer's disease. *Ann Neurol* **45**, 358–368 (1999).
10. Neuropathology, G. Pathological correlates of late-onset dementia in a multicentre, community-based population in England and Wales. Neuropathology Group of the Medical Research Council Cognitive Function and Ageing Study (MRC CFAS). *Lancet* **357**, 169–175 (2001).
11. Snowdon, D. A. Healthy aging and dementia: findings from the Nun Study. *Ann Intern Med* **139**, 450–454 (2003).

12. Stern, Y. *et al*. Influence of education and occupation on the incidence of Alzheimer's disease. *Jama* **271**, 1004–1010 (1994).
13. Tucker, A. M. & Stern, Y. Cognitive reserve in aging. *Curr Alzheimer Res* **8**, 354–360 (2011).
14. Whalley, L. J. *et al*. Childhood mental ability and dementia. *Neurology* **55**, 1455–1459 (2000).
15. Andrade-Moraes, C. H. *et al*. Cell number changes in Alzheimer's disease relate to dementia, not to plaques and tangles. *Brain* **136**, 3738–3752 (2013).
16. Perez-Nievas, B. G. *et al*. Dissecting phenotypic traits linked to human resilience to Alzheimer's pathology. *Brain* **136**, 2510–2526 (2013).
17. Sofroniew, M. V. & Vinters, H. V. Astrocytes: biology and pathology. *Acta Neuropathol* **119**, 7–35 (2010).
18. Medeiros, R. & LaFerla, F. M. Astrocytes: conductors of the Alzheimer disease neuroinflammatory symphony. *Exp Neurol* **239**, 133–138 (2013).
19. Belanger, M. & Magistretti, P. J. The role of astroglia in neuroprotection. *Dialogues Clin Neurosci* **11**, 281–295 (2009).
20. Mathur, R. *et al*. A reduced astrocyte response to beta-amyloid plaques in the ageing brain associates with cognitive impairment. *PLoS One* **10**, e0118463 (2015).
21. Doody, R. S. *et al*. Phase 3 trials of solanezumab for mild-to-moderate Alzheimer's disease. *N Engl J Med* **370**, 311–321 (2014).
22. Hughes, C. P., Berg, L., Danziger, W. L., Coben, L. A. & Martin, R. L. A new clinical scale for the staging of dementia. *Br J Psychiatry* **140**, 566–572 (1982).
23. Jellinger, K. A. Clinicopathological analysis of dementia disorders in the elderly–an update. *J Alzheimers Dis* **9**, 61–70 (2006).
24. Morris, J. C. The Clinical Dementia Rating (CDR): current version and scoring rules. *Neurology* **43**, 2412–2414 (1993).
25. Montine, T. J. *et al*. National Institute on Aging-Alzheimer's Association guidelines for the neuropathologic assessment of Alzheimer's disease: a practical approach. *Acta Neuropathol* **123**, 1–11 (2012).
26. Farfel, J. M. *et al*. Very low levels of education and cognitive reserve: a clinicopathologic study. *Neurology* **81**, 650–657 (2013).
27. Ferretti-Rebustini, R. E. *et al*. Validity of the Katz Index to assess activities of daily living by informants in neuropathological studies. *Rev Esc Enferm USP* **49**, 946–952 (2015).
28. Ferretti, R. *et al*. Post-Mortem diagnosis ofdementia by informant interview. *Dement Neuropsychol* **4**, 138–144 (2010).
29. Marra, T. A., Pereira, D. S., Faria, C. D., Tirado, M. G. & Pereira, L. S. Influence of socio-demographic, clinical and functional factors on the severity of dementia. *Arch Gerontol Geriatr* **53**, 210–215 (2011).
30. Glei, D. A. *et al*. Participating in social activities helps preserve cognitive function: an analysis of a longitudinal, population-based study of the elderly. *Int J Epidemiol* **34**, 864–871 (2005).
31. Zarow, C. *et al*. Correlates of hippocampal neuron number in Alzheimer's disease and ischemic vascular dementia. *Ann Neurol* **57**, 896–903 (2005).
32. Du, A. T. *et al*. Magnetic resonance imaging of the entorhinal cortex and hippocampus in mild cognitive impairment and Alzheimer's disease. *J Neurol Neurosurg Psychiatry* **71**, 441–447 (2001).
33. Vasile, F., Dossi, E. & Rouach, N. Human astrocytes: structure and functions in the healthy brain. *Brain Struct Funct* **222**, 2017–2029 (2017).
34. Yassa, M. A., Muftuler, L. T. & Stark, C. E. Ultrahigh-resolution microstructural diffusion tensor imaging reveals perforant path degradation in aged humans *in vivo*. *Proc Natl Acad Sci USA* **107**, 12687–12691 (2010).
35. McCall, M. A. *et al*. Targeted deletion in astrocyte intermediate filament (Gfap) alters neuronal physiology. *Proc Natl Acad Sci USA* **93**, 6361–6366 (1996).
36. Sovrea, A. S. & Bosca, A. B. Astrocytes reassessment - an evolving concept part one: embryology, biology, morphology and reactivity. *J Mol Psychiatry* **1**, 18 (2013).
37. Steiner, J. *et al*. Evidence for a wide extra-astrocytic distribution of S100B in human brain. *BMC Neurosci* **8**, 2 (2007).
38. Boyes, B. E., Kim, S. U., Lee, V. & Sung, S. C. Immunohistochemical co-localization of S-100b and the glial fibrillary acidic protein in rat brain. *Neuroscience* **17**, 857–865 (1986).
39. Pekny, M. & Pekna, M. Astrocyte reactivity and reactive astrogliosis: costs and benefits. *Physiol Rev* **94**, 1077–1098 (2014).
40. Hamby, M. E. & Sofroniew, M. V. Reactive astrocytes as therapeutic targets for CNS disorders. *Neurotherapeutics* **7**, 494–506 (2010).
41. Morimoto, K. *et al*. Expression profiles of cytokines in the brains of Alzheimer's disease (AD) patients compared to the brains of non-demented patients with and without increasing AD pathology. *J Alzheimers Dis* **25**, 59–76 (2011).
42. Zorec, R., Horvat, A., Vardjan, N. & Verkhratsky, A. Memory Formation Shaped by Astroglia. *Front Integr Neurosci* **9**, 56 (2015).
43. Pekny, M., Wilhelmsson, U. & Pekna, M. The dual role of astrocyte activation and reactive gliosis. *Neurosci Lett* **565**, 30–38 (2014).
44. Danbolt, N. C. Glutamate uptake. *Prog Neurobiol* **65**, 1–105 (2001).
45. Rothstein, J. D. *et al*. Localization of neuronal and glial glutamate transporters. *Neuron* **13**, 713–725 (1994).
46. Sosunov, A. A., Guilfoyle, E., Wu, X., McKhann, G. M. 2nd & Goldman, J. E. Phenotypic conversions of "protoplasmic" to "reactive" astrocytes in Alexander disease. *J Neurosci* **33**, 7439–7450 (2013).
47. Masliah, E., Alford, M., DeTeresa, R., Mallory, M. & Hansen, L. Deficient glutamate transport is associated with neurodegeneration in Alzheimer's disease. *Ann Neurol* **40**, 759–766 (1996).
48. Mookherjee, P. *et al*. GLT-1 loss accelerates cognitive deficit onset in an Alzheimer's disease animal model. *J Alzheimers Dis* **26**, 447–455 (2011).
49. Zumkehr, J. *et al*. Ceftriaxone ameliorates tau pathology and cognitive decline via restoration of glial glutamate transporter in a mouse model of Alzheimer's disease. *Neurobiol Aging* **36**, 2260–2271 (2015).
50. Saur, L. *et al*. Physical exercise increases GFAP expression and induces morphological changes in hippocampal astrocytes. *Brain Struct Funct* **219**, 293–302 (2014).
51. Viola, G. G. *et al*. Morphological changes in hippocampal astrocytes induced by environmental enrichment in mice. *Brain Res* **1274**, 47–54 (2009).
52. Wang, X. *et al*. Pre-ischemic treadmill training alleviates brain damage via GLT-1-mediated signal pathway after ischemic stroke in rats. *Neuroscience* **274**, 393–402 (2014).
53. Choi, M. *et al*. Hippocampus-based contextual memory alters the morphological characteristics of astrocytes in the dentate gyrus. *Mol Brain* **9**, 72 (2016).
54. Sugishita, M. & Furukawa, K. Clinical Dementia Rating (CDR). *Nihon Rinsho* **69** Suppl 8, 413–417 (2011).
55. Katz, S., Ford, A. B., Moskowitz, R. W., Jackson, B. A. & Jaffe, M. W. studies of illness in the aged. the index of adl: a standardized measure of biological and psychosocial function. *Jama* **185**, 914–919 (1963).
56. Lawton, M. P. & Brody, E. M. Assessment of older people: self-maintaining and instrumental activities of daily living. *Gerontologist* **9**, 179–186 (1969).
57. Thal, D. R., Rub, U., Orantes, M. & Braak, H. Phases of A beta-deposition in the human brain and its relevance for the development of AD. *Neurology* **58**, 1791–1800 (2002).
58. Braak, H. & Braak, E. Neuropathological stageing of Alzheimer-related changes. *Acta Neuropathol* **82**, 239–259 (1991).
59. Braak, H., Alafuzoff, I., Arzberger, T., Kretzschmar, H. & Del Tredici, K. Staging of Alzheimer disease-associated neurofibrillary pathology using paraffin sections and immunocytochemistry. *Acta Neuropathol* **112**, 389–404 (2006).
60. Mirra, S. S. *et al*. The Consortium to Establish a Registry for Alzheimer's Disease (CERAD): Part II. Standardization of the neuropathologic assessment of Alzheimer's disease. *Neurology* **41**, 479–479 (1991).

Acknowledgements
The authors would like to thank Kozue Kamiya, Yuko Hayakawa, and Tatsuya Shiraishi for technical support, Natsumi Hashimoto, Mami Yamaguchi and Michitoshi Kimura for support with cutting paraffin sections and Bielschowsky staining, Kota Iwamura for support of brain fixation. This work was supported by JSPS KAKENHI Grant Number JP16K19317 and LEOC Co., Ltd. There is no financial relationship to disclose.

Author Contributions
E.K., M.N. and M.F. designed the study and wrote the paper. S.M. assisted brain removal and fixation. K.K., N.H., T.C., M.O., Y.M. and K.N. helped analysis of the data.

Additional Information
Supplementary information accompanies this paper at https://doi.org/10.1038/s41598-018-19442-7.

Competing Interests: The authors declare that they have no competing interests.

Publisher's note: Springer Nature remains neutral with regard to jurisdictional claims in published maps and institutional affiliations.

Supplementary information

1. Supplementary Tables
2. Supplementary Figures
3. Methods
4. References

Activated forms of astrocytes with higher GLT-1 expression are associated with cognitive normal subjects with Alzheimer pathology in human brain

Eiji Kobayashi, Masako Nakano, Kenta Kubota, Nobuaki Himuro, Shougo Mizoguchi, Takako Chikenji, Miho Otani, Yuka Mizue, Kanna Nagaishi, Mineko Fujimiya

Supplementary Table 1. Characteristics of subjects

	N-N (n=19)	AD-N (n=10)	AD-D (n=18)	Total (n=47)
Cause of death, n (%)				
Heart failure, vascular disease	7	3	3	13 (28%)
Carcinoma	6	2	-	8 (17%)
Senility death	1	1	6	8 (17%)
Pneumonia	4	-	2	6 (13%)
Septicemia	-	2	2	4 (9%)
Digestive disease	1	1	1	3 (6%)
Kidney failure	-	1	-	1 (2%)
other	-	-	1	1 (2%)
Living location*, n (%)				
Home	16	8	3	27 (57%)
Nursing home	2	1	13	16 (34%)
Hospital	1	1	2	4 (9%)

* Information at 6month before death.

Supplementary Table 2. Characteristics of informants

	N-N (n=19)	AD-N (n=10)	AD-D (n=18)	Total (n=47)
Age	68±12.6	65.5±17.7	67.5±15.9	67±12.1
Sex, n				
Male	1	2	8	11(23%)
Female	18	8	10	36 (77%)
Relations with subjects, n (%)				
child, grandchild	13	5	6	24 (49%)
spouse	13	3	3	19 (40%)
nephew, niece	-	2	5	7 (15%)
brother, sister	1	-	4	5 (11%)
others	2		-	2 (4%)
Contact with subjects*, n (%)				
everyday	13	5	6	24 (49%)
3~4days/week	1	1	1	3 (6%)
1~2days/week	2	1	1	4 (9%)
less than one day/week	3	3	10	16 (34%)
post mortem interval, days	447.7±219	419.8±199	421.5±212.4	429.7±210.1

* Information at 6month before death.

Supplementary Table 3. Number of subjects classified in each criteria of AD neuropathological diagnosis by dementia status.

AD neuropathological diagnosis	No Dementia (n=29)	Dementia (n=18)
"A" Thal Aβ phase		
0	15 (34%)	0
1	2 (7%)	0
2	3 (10%)	1 (5%)
3	6 (21%)	12 (67%)
4	2 (7%)	0
5	1 (3%)	5 (28%)
"B" Braak NFT stage		
Ⅰ	12 (41%)	0
Ⅱ	4 (14%)	0
Ⅲ	7 (24%)	6 (33%)
Ⅳ	5 (17%)	7 (39%)
Ⅴ	1 (3%)	4 (22%)
Ⅵ	0	1 (6%)
"C" CERAD neuritic plaque score		
None	18 (62%)	0
Sparse	1 (4%)	3 (17%)
Moderate	9 (30%)	11 (61%)
Frequent	1 (4%)	4 (22%)

Supplementary Figure 1.

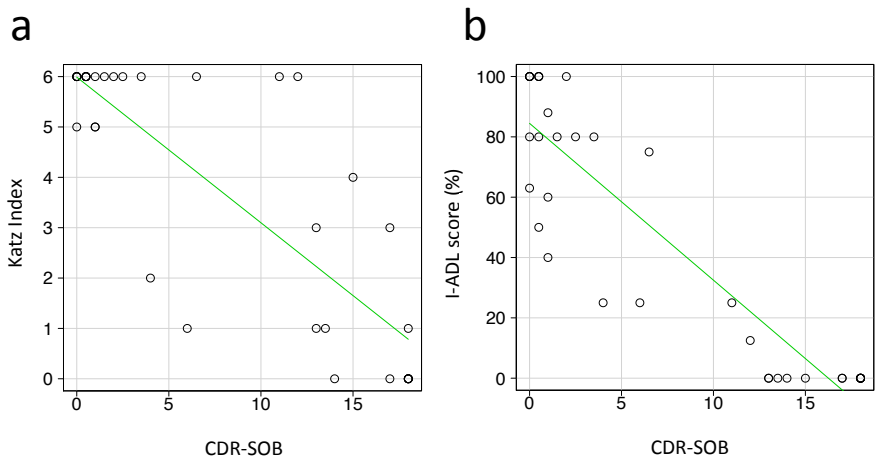

Supplementary Figure 1. Factors correlated with CDR-SOB. Factors well correlated with CDR-SOB are (a) Katz Index (rs = -0.73, $P < 0.001$) and (b) I-ADL score (rs = -0.79, $P < 0.001$). (rs: Spearmann's rank correlation coefficient).

Supplementary Figure 2.

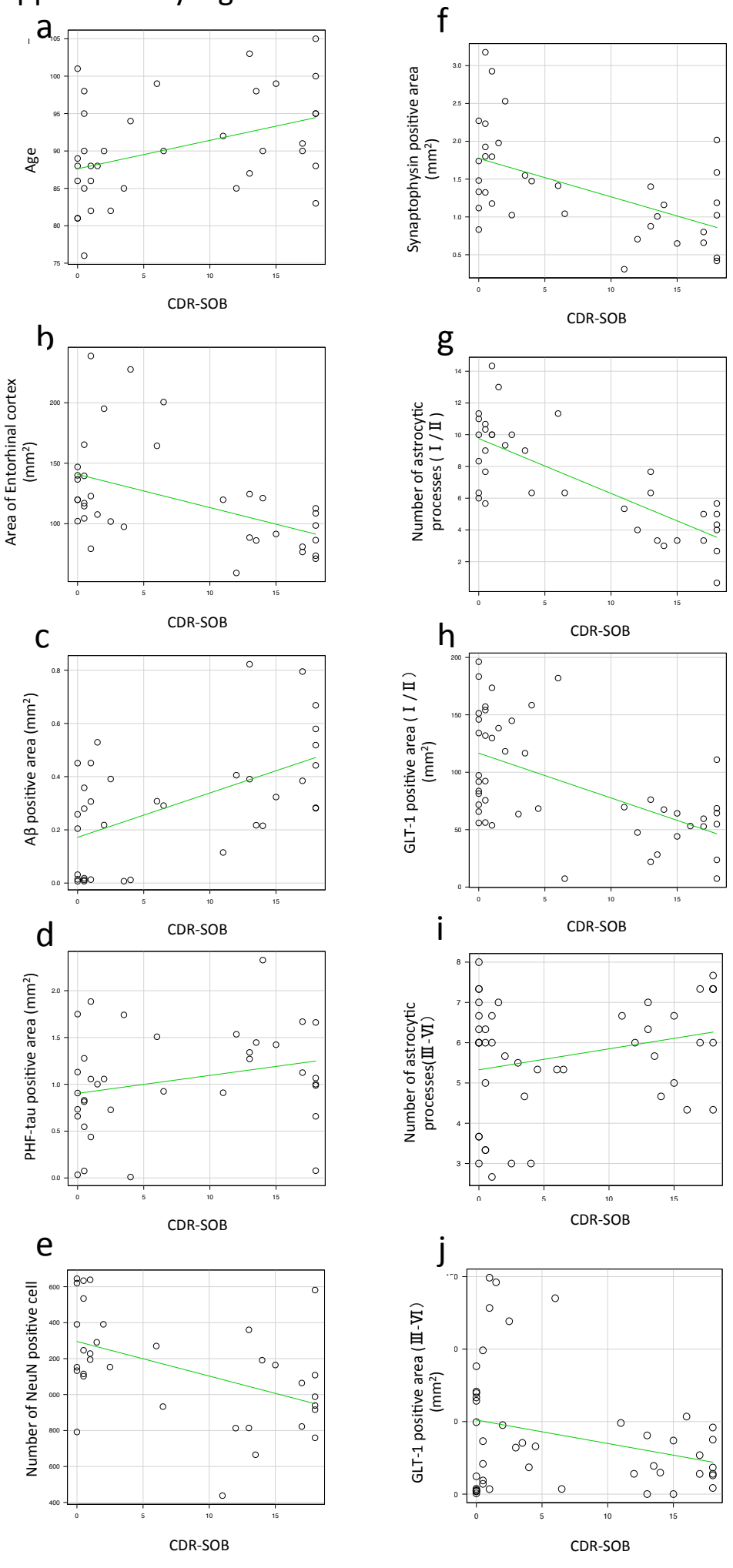

Supplementary Figure 2. Correlations between other factors and CDR-SOB. The factors correlated with CDR-SOB include (a) age (rs = -0.4, $P < 0.05$), (b) area of the EC (rs = -0.51, $P < 0.01$), (c) Aβ-positive area (rs = 0.51, $P < 0.01$), (d) PHF-tau-positive area (rs = 0.21, n.s), (e) number of NeuN-positive cells (rs = -0.44, $P < 0.01$), (f) synaptophysin positive area (rs = 0.48, $P < 0.01$), (g) number of astrocytic processes (I/II) (rs = -0.71, $P < 0.001$), and (h) GLT-1-positive area (I/II) (rs = -0.57, $P < 0.001$,(i) number of astrocytic processes (III-VI) (rs = -0.09, n.s), and (h) GLT-1-positive area (III-VI) (rs = -0.09, n.s). (rs: Spearmann's rank correlation coefficient).

Supplementary Figure 3.

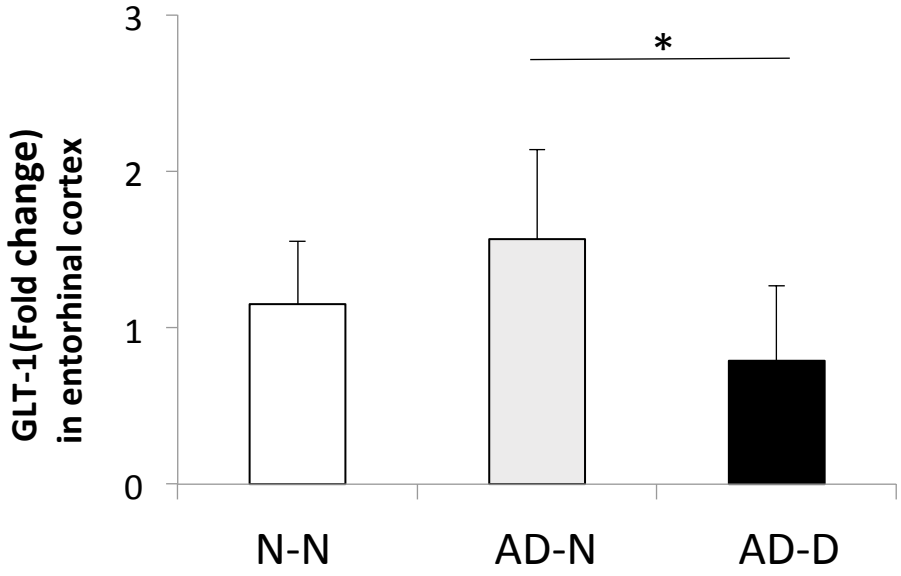

Supplementary Figure 3. The mRNA expression for GLT-1 in layer I and II of the entorhinal cortex (EC) was lower in the AD-D group than in the AD-N group. No difference was found between the AD-D and N-N groups. *$P < 0.05$, one-way ANOVA, Tukey post-test. Values are means ± SD (N-N: n=6, AD-N: n=6, AD-D: n=6).

Supplementary Figure 4.

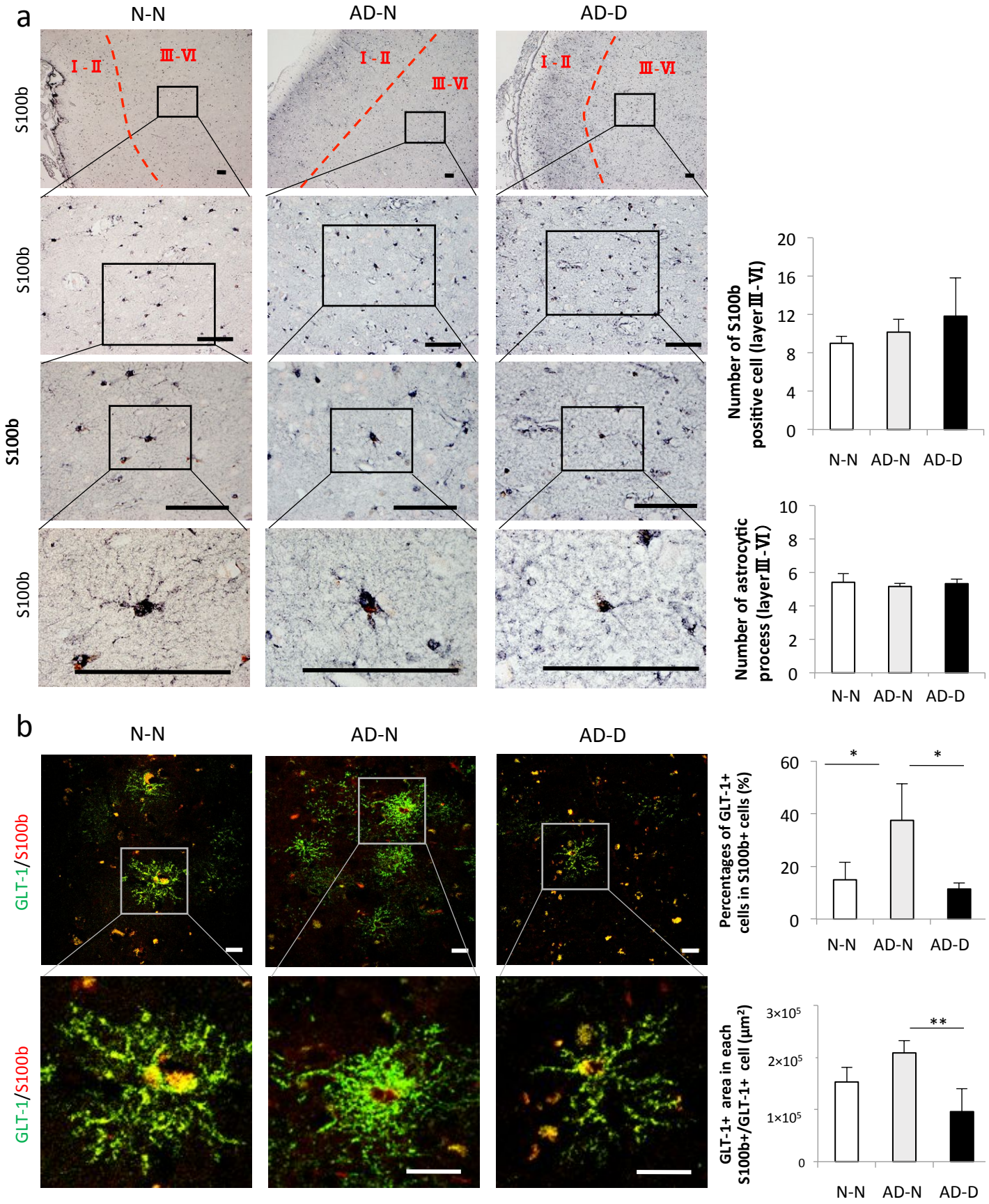

Supplementary Figure 4. Immunohistochemical analysis of S100b and GLT-1 in layer III-VI of EC. (**a**) Images of S100b-positive cells shown at different magnifications (Bar = 100 μm). No significant difference is found in the number of S100b-positive cells and the number of cell processes observed 20 μm away from the soma among the three groups. Values are means ± SD (N-N: n=19, AD-N: n=10, AD-D: n=18). (**b**) Overlap staining with GLT-1 and S100b images are shown (Bar = 20 μm). The percentages of GLT-1-positive cells in S100b-positive cells in the layer III-VI of the EC is higher in the AD-N group than in the N-N and the AD-N groups, while no difference is found between the AD-D and N-N groups. The GLT-1-positive area in each GLT-1/S100b-positive cells, which are stained with S100b in perikarya and stained with GLT-1 in the distal cell processes, is lower in the AD-D group than in the AD-N group, while no difference is found between the AD-D and N-N groups. **P* <0.05, ** *P* < 0.01, one-way ANOVA, Tukey post-test. Values are means ± SD (N-N: n=4, AD-N: n=4, AD-D: n=4).

Methods.

Exclusion criteria.

To exclude neurological disease other than AD as far as possible, we set the following exclusion criteria, 1) brains with macroscopic infarction or hemorrhage (> 10mm), 2) subjects with a past history of cerebrovascular disease, mental disorders or neurological deficits except AD (e.g., depression, Lewy body disease), and 3) subjects for whom a CDR score was difficult to ascertain (e.g., a lack of information).

Questionnaires.

Questionnaires were completed by bereaved family members or other acquaintances of the deceased (Supplementary table 2). Where items in the questionnaires were unclear, an additional interview was carried out by telephone. The score of CDR show the diverse of cognitive function as absent, questionable, mild, moderate, or severe (CDR 0, 0.5, 1, 2, 3 respectively)[1-3]. In present study, "No dementia" was determined as a CDR score of 0 or 0.5, and "Dementia" was determined as a CDR score of 1, 2 or 3 for convenience as previously reported[1,2,4]. The CDR score was assessed by two evaluators (E.K and M.N) independently, and the inter-rater reliability of this test was very high (Kendall's rank correlation tau = 0.9, $P < 0.001$). In addition, the CDR Sum of Boxes (CDR-SOB) was calculated as reported previously[5]. All informants were asked to provide information on the donors at 6 months prior to death. Additional information including past medical history, years of education and address at 6 months before death was obtained from the questionnaires. The cause of death was also confirmed from the Certificate of Death in each case (Supplementary Table 1).

AD neuropathological diagnosis.

Brains were removed and fixed in 10% formalin. The left hemispheres were removed and cut into blocks to provide 5 to 10mm coronal sections. We obtained sections for 8 areas of each brain: (1) hippocampus and entorhinal cortex, (2) middle frontal gyrus, (3) superior and middle temporal gyrus, (4) inferior parietal lobule, (5) occipital cortex (BA 17 and 18), (6) midbrain (including the Substantia nigra), (7) cerebellum cortex and dentate nucleus, and (8) basal ganglia with basal nucleus of Mynert, based on previous reports[6].

For evaluation of Thal Phase, Aβ immunohistochemical analysis was performed for each area. Phase 0 denotes the absence of Aβ deposits in any area; phase 1 was characterized by deposits exclusively in the neocortex; phase 2 by additional involvement of the allocortex including CA1 and the entorhinal region; phase 3 by further deposits in the subcortical region including the basal ganglia, and phase 4 and 5 by additional deposits in the midbrain and cerebellum, respectively. After Thal Phase evaluation, we assessed the "A" in the "ABC score," which is limited to four stages (A0 corresponds to Phase 0, A1 includes Phase 1 and 2, A2 corresponds to Phase 3, and A3 includes Phase 4 and 5).

For evaluation of the Braak stage, we undertook phospho-tau immunohistochemical analysis for each area[6]. Stage I was characterized by NFTs in the transentorhinal region of the hippocampus; stage II by extended NFTs in the entorhinal cortex region of the hippocampus; stage III by further extension in the fusiform in the temporal cortex and lingual gyri in the occipital cortex; stage IV by increased NFT density in the sites affected in stage III; stage V by extension of the neocortical NFTs into the frontal and superior temporal gyrus; and stage VI by severe involvement of most areas of the neocortex and extension into the striate area. After evaluation of the Braak stage, we assessed the "B" in the "ABC score," which is again limited to four stages (B0 corresponds to None, B1 includes Stage I and II, B2 includes Stage III and IV, and B3 includes Stage V and VI).

For evaluation of the CERAD score, we performed Bielschowsky staining of the neocortical area as described previously[6,7]. No neuritic plaques was scored as "None;" an increasing density of plaques (1 to 5 plaques per 1 mm^2) was scored as "Sparse;" and an even greater plaque density was determined as "Moderate" or "Frequent" (6 to 20 plaques or over 20 plaques per 1 mm^2, respectively). After evaluation of the CERAD score, we assessed the "C" in the "ABC score," which consists of four stages (C0 corresponds to "None", C1 to "Sparse", C2 to "Moderate", and C3 to "Frequent").

Macroscopic assessment of the EC.

We scanned the coronal sections of the left hemisphere that include the lateral geniculate body and hippocampus by digital scanner. The area of the EC was then evaluated by Image J as reported previously[8].

Immunohistochemistry.

The sections were incubated for 2 days at 4 ^oC with primary antibodies against beta-amyloid (D54D2) (rabbit mAb, 1:100; Cell signaling, Danvers, MA, USA), PHF-tau (Anti-Human Monoclonal, 1:80; Thermo Fisher Scientific, Waltham, MA, USA), NeuN (rabbit polyclonal, 1:250; Millipore, Darmstadt, Germany), synaptophysin (rabbit polyclonal, 1:250; Sigma-Aldrich, St. Louis, MO, USA), GFAP (chicken polyclonal, 1:500; Millipore), S100b (rabbit polyclonal, 1:200; abcam, Cambridge, UK), and GLT-1 (mouse GLT-1, 1:100; FRONTIER INSTITUTE, Hokkaido, Japan). After blocking with 0.1% H_2O_2, sections were incubated with biotinylated secondary antibodies, anti-rabbit IgG (1:1000; Jackson ImmunoResearch, West Grove, PA, USA), anti-mouse IgG (1:1000; Jackson ImmunoResearch) and anti-chiken IgY (1:1000; Jackson ImmunoResearch), for 2h at room temperature. Sections were incubated in AB complex for 1.5h at room temperature, and then DAB solution mixed with 1% H_2O_2 and Nickel Ammonium Sulfate was added to each section, which were then further incubated for 60 min at room temperature. Finally, nuclei were stained with neutral red.

Quantitative analysis of DAB staining.

Quantitative analysis was performed on the EC. The area positive for Aβ and PHF-tau was evaluated in 6 different fields in layer I -VI per brain (3 fields of 3.2 × 2.4 mm per section). The number of NeuN-positive cells and the area of synaptophysin were evaluated in 6 different fields in layer of I -VI per brain (3 fields of 3.2 × 2.4 mm per section). The area positive for GFAP was evaluated in 6 different fields in layer I/II and layer III-VI each, per brain (3 fields of 1280 × 960 μm per section). The number of GFAP-positive cells were counted in 6 different fields in layer I/II and layer III-VI each, per brain (3 fields of 150×150 μm per section). The number of the astrocytic processes observed 20 μm away from the soma was counted in 12 different cells in layer I/II and layer III-VI each, per brain (6 cells per section) by Sholl analysis[9]. The number of S100b-positive cells were counted in 6 different fields in layer III-VI each, per brain (3 fields of 150×150 μm per section). The number of the S100b-positive cell processes observed 20 μm away from the soma was counted in 12 different cells in layer III-VI each, per brain (6 cells per section) by Sholl analysis[9]. The area positive for GLT-1 was also evaluated in 6 different fields in layer I/II and layer III-VI each, per brain (3 fields of 640 × 480 μm per section).

All sections were assessed by light microscopy (Nikon Eclipse), and NIS-Elements software 3.22.00 (Nikon) was used to obtain images. All immunohistochemical analyses were performed using Image J 1.5 (National Institute of Health) after binarization.

Immunofluorescences staining.

For immunofluorescence staining analysis, coronal sections were cut into 5μm thick paraffin-embedded sections and obtained every 25μm. The sections were incubated for 2 days at 4℃ with primary antibodies against S100b (rabbit polyclonal, 1:200; abcam) and GLT-1 (guinea pig polyclonal, 1:100; FRONTIER INSTITUTE). For secondary antibodies, Cy3-labeled anti-rabbit IgG (Jackson ImmunoResearch,) and Alexa Fluor 488-labeled anti-guinea pig IgG (Millipore) diluted in 1:500 were used. Sections were observed under confocal laser scanning microscopy (Nikon A1, Tokyo, Japan).

The percentage of GLT-1-positive cells in S100b-positive cells were evaluated in the layer III-VI of EC. The GLT-1-positive area in each GLT-1/ S100b-poitive cells were evaluated in 4 different cells in layer III to VI each, per brain. The GLT-1/ S100b- positive cells were defined as the cells which were stained with S100b in perikarya and stained with GLT-1 in the distal cell processes.

Total RNA isolation, Reverse transcription (RT) and real time RT-PCR

Total RNA was isolated from the area of layer I/II in entorhinal cortex which is paraffin-embedded sections by using the Invitrogen Recover All™ Total Nucleic Acid Isolation kit (Thermo Fisher Scientific). The complementary DNA (cDNA) was synthesized by using a Sensiscript Reverse Transcriptase (RT) Kit (QIAGEN, Hilden, Germany), and mRNA levels were measured by RT-PCR using Power SYBR Green PCR Master Mix (Thermo Fisher Scientific). GLT-1 mRNA was detected by primers: GGGCTTCTTCGCTTGGCATCTC (forward) and CTCCGGCACCTCAGTCACAGTC (reverse). Glyceraldehyde-3-phosphate dehydrogenase (GAPDH) mRNA was detected as an internal standard with primers: ATTGCCCTCAACGACCACTT (forward) and TGCTGTAGCCAAATTCGTTGTC (reverse). The relative changes in gene expression was determined by the $2^{-\Delta\Delta Ct}$ method.

References

1. Hughes, C. P., Berg, L., Danziger, W. L., Coben, L. A. & Martin, R. L. A new clinical scale for the staging of dementia. Br J Psychiatry 140, 566-572 (1982).
2. Morris, J. C. The Clinical Dementia Rating (CDR): current version and scoring rules. Neurology 43, 2412-2414 (1993).
3. Sugishita, M. & Furukawa, K. [Clinical Dementia Rating (CDR)]. Nihon Rinsho 69 Suppl 8, 413-417 (2011).
4. Jellinger, K. A. Clinicopathological analysis of dementia disorders in the elderly--an update. J Alzheimers Dis 9, 61-70 (2006).
5. O'Bryant, S. E. et al. Staging dementia using Clinical Dementia Rating Scale Sum of Boxes scores: a Texas Alzheimer's research consortium study. Arch Neurol 65, 1091-1095 (2008).
6. Montine, T. J. et al. National Institute on Aging-Alzheimer's Association guidelines for the neuropathologic assessment of Alzheimer's disease: a practical approach. Acta Neuropathol 123, 1-11 (2012).
7. Mirra, S. S. et al. The Consortium to Establish a Registry for Alzheimer's Disease (CERAD): Part II. Standardization of the neuropathologic assessment of Alzheimer's disease. Neurology 41, 479-479 (1991).
8. Mizutani, T. & Kasahara, M. Hippocampal atrophy secondary to entorhinal cortical degeneration in Alzheimer-type dementia. Neurosci Lett 222, 119-122 (1997).
9. Wilhelmsson, U. et al. Redefining the concept of reactive astrocytes as cells that remain within their unique domains upon reaction to injury. Proc Natl Acad Sci U S A 103, 17513-17518 (2006).